Design Optimization Study of Fault Tolerant and Redundant Motor Drivetrains for Urban Air Mobility Vehicles

Thomas Francis Tallerico Rotating and Drives Systems Branch NASA Glenn Research Center Cleveland, Ohio thomas.tallerico@nasa.gov Andrew Douglas Smith Thermal Branch NASA Glenn Research Center Cleveland, Ohio andrew.d.smith-1@nasa.gov Jeffryes Walter Chapman Systems Analysis Branch NASA Glenn Research Center Cleveland, Ohio jeffryes.w.chapman@nasa.gov

Abstract— Fully electric and hybrid electric aircraft will require extremely lightweight and reliable electric motor drivetrains to meet performance and safety goals. It is likely that to meet reliability targets some form of fault tolerance and/or redundancy will need to be used in the electric motor drivetrain. The use of either redundancy or fault tolerance will result in a reduction in drivetrain performance. In this paper, an example design study is carried out comparing redundant and fault tolerant drivetrains based on an example fault tolerant motor topology for a tilt rotor UAM application. Results show a minimal weight penalty for the incorporation of fault tolerance into drivetrains with the example motor explored here.

I. INTRODUCTION

Fully electric and hybrid electric aircraft require high performance and reliable electric motor drivetrains. Presently, defining electric motor reliability with sufficient certainty to meet aviation standards is difficult due to the lack of motor winding lifetime models and data relevant to aircraft propulsion applications [1]. As a result, it is likely that electric and hybrid electric aircraft will have to use some form of redundancy or fault tolerance in their motor drivetrains to meet minimum safety standards. Both the use of redundant propulsors or a fault tolerant motor drivetrain to meet safety standards requires an overdesign of the system to meet engine out or faulted operation power requirements. The overdesign of the system results in mass and/or loss penalties for the aircraft in nominal operation.

This paper presents example design studies of fault tolerant and redundant motor drivetrains for urban air mobility applications. The fault tolerant motor drivetrain is based on the work of Swanke et al [2] [3] [4]. The motor topology, depicted in Fig 1, has four modules and includes features to maximize galvanic, magnetic, and thermal isolation between phases and modules in the machine. For the comparison redundant propulsor motor drivetrains, the same nominal machine design is used but without fault tolerant features.

This paper is organized such that Section II discusses the study assumptions, Section III presents the design methodology, Section IV presents the study results, and Section V provides a conclusion.

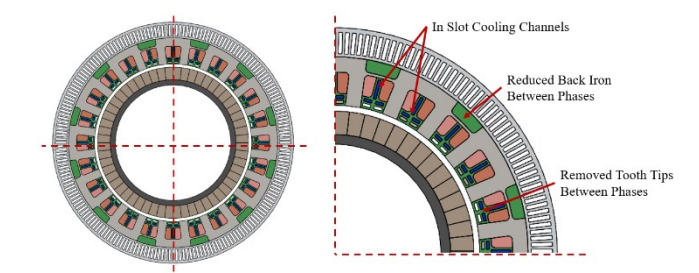


Figure 1 Fault Tolerant Machine Geometry Based on [4]
Table 1 Mission Profile Definitions for Design Studies

Nominal Mission						
Mission Point	Duration	Powers				
Hover	40 s	100 kW				
Climb	4 min	105 kW				
Cruise	20 min	51 kW				
Hover	40 s	100 kW				
Faulted Mission						
Mission Point	Duration	Powers				
		Fault Tolerant	Redundant			
Hover	40 s	100 kw	100 kw			
Climb	4 min	105 kW	105 kW			
Cruise	20 min	51 kW (with fault)	51 kW * Rotors Rotors-2			
Hover	2 min	100 kW (with fault)	100 kW * Rotors Rotors - 2			

II. DESIGN STUDY ASSUMPTIONS

The design studies are carried out for a tilt rotor UAM vehicle. The assumed mission profile of the vehicle is based on one half of the double hop mission from [5]. The assumed design mission is summarized in Table 1 for both the fault tolerant and redundant propulsor motor drivetrains. A tilt rotor vehicle topology was selected because its ratio of climb to hover power makes engine out hover conditions the peak power case for the motor [6].

It is assumed that in the event of a motor winding failure, the vehicle will fly at cruise power to a landing location and hover to land. Excess landing hover time is added to the mission profiles with a failure. As a worst case relative to the assumed operations under motor winding failure, the failures are assumed to happen at the top of climb when the motor is already at its

hottest point. For the fault tolerant motor drivetrains, the worst case fault is assumed to be a turn-to-turn fault across a single turn.

The bulk of the assumptions related to the materials used and constraints on the designs can be found in [6] and [7]. The rotors/fans on each propulsor are assumed to rotate at 1 krpm and collective control is assumed such that motor rotational speed is constant throughout the mission.

III. DESIGN METHODOLOGY

The design optimization methodology is based on an updated version of the UAM motor design optimization tool presented in [7]. The tool is focused on motor design but includes gearbox, inverter, and thermal management system (TMS) design in order to constrain the motor optimization and estimate total drivetrain weight and power consumption. Fig 2 shows a flow diagram of the tool used in this paper.

The design tool uses a genetic optimizer wrapped around sequential optimizations of the gearbox, motor, inverter, and thermal management system. The following sections provide brief descriptions of each analysis used in the design optimization process. Table 2 lists the optimization variables used. Seven variables are used to define redundant propulsion drivetrains. Two additional, tooth tip gap and in-slot cooling width, are used to define the fault tolerant machines, because these two variables contribute to the magnitude of the faulted current and the thermal isolation between adjacent coils. The fitness of each set of genes selected by the optimizer is evaluated through 12 sequential analyses/optimizations.

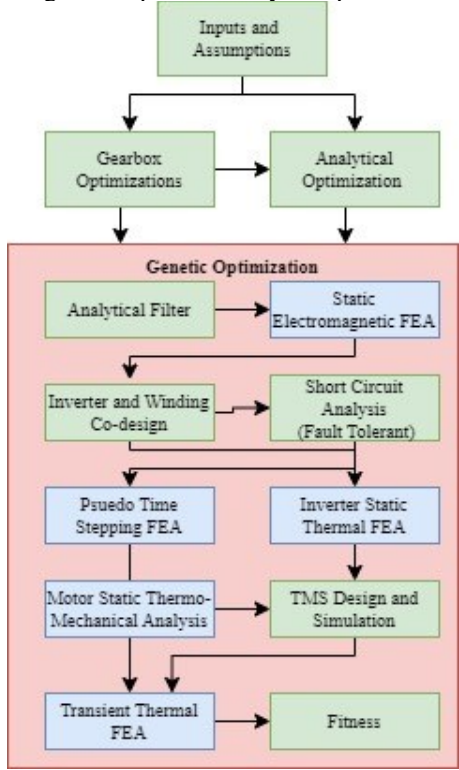


Figure 2 Design Tool Flow Diagram

TT 11 3	<i>a</i>	0		T7 · 11
Table 2	Tenetic	(Infimi	zation	Variables

Electrical Frequency	Motor Rotor Radius			
Inverter Mass Target	Gearbox Specific Torque Index			
Motor Mass Target	Coolant Volumetric Flow Rate			
Motor Magnet Thickness	Motor Tooth Tip Gap (Fault Tolerant Only)			
Motor In-Slot Cooling Width (Fault Tolerant Only)				

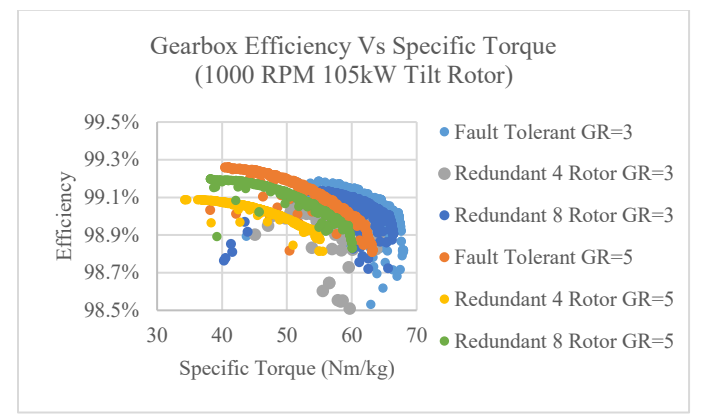


Figure 3 Gearbox Performance Optimization Results at GR=3 and GR=5 for the Different Studies

A. Gearbox

For each design case gearbox mass, efficiency, and gear ratio trades are estimated using the methodology described in [8]. Gearboxes are preoptimized and then curve fits are used to turn the data into a scattered interpolant function that estimates efficiency as a function of gear ratio and gearbox specific torque index. Gear ratio indirectly and specific torque index directly are controlled by the genetic optimizer.

For the fault tolerant motor drivetrain, gearboxes are sized for 5000 hours with 99.9% reliability at peak nominal mission power. Redundant propulsor drivetrains are sized for a total life of 5000 hours assuming 99.9% of the lifetime is spent at peak nominal mission power and 0.1% of the lifetime is spent in the engine out condition as defined in Table 1.

Gearbox efficiency vs specific torque results for the different cases used in this paper are shown in Fig 3. Only gear ratio 3 and 5 results are shown for clarity and because they are most relevant to the results in section IV where optimal motor rpm fell in the range of 3-7 krpm. Gearbox data up to a gear ratio of 30 was included in the design optimizations.

B. Analytical Sizing

An analytical evaluation of drivetrain performance is included in the optimization to generate a good initial population, filter out bad designs selected by the genetic optimizer with minimal computational cost, and generate initial stator geometry for the FEA models of the motor. The model uses the gearbox, inverter, and TMS analytical design portions of the higher fidelity design tool and an analytical model of the motor as was described in [6] [7].

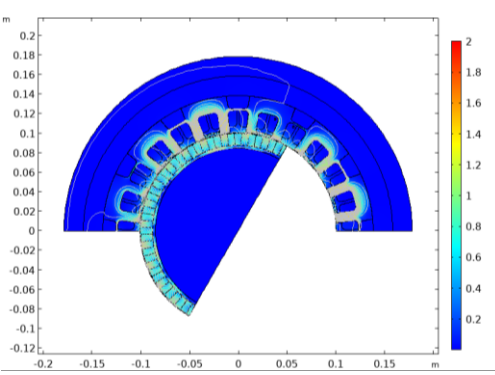


Figure 4 Example Electromagnetic FEA and Result

C. Motor Static FEA

Using the motor geometry generated by the genetic optimizer and the analytical sizing of the machine, a sweep of current amplitude from 0 to 30 A/mm² is carried out in static FEA. Torque and stator iron magnetic field data vs stator current is extracted from the model and used to resize the stator geometry to maximize thermal performance and the efficiency of the machine at the mass specified by the genetic optimizer as was described in [7]. Required current at each mission design point for the new geometry is estimated.

The new geometry is simulated with the design point currents using static magnetic FEA. Magnetic field, torque, and coil inductance data are extracted from the results. For the fault tolerant motor case, additional current steps are included to capture the phase to phase mutual inductance and the single turn to phase mutual inductance of the motor to enable single turn faulted current estimation. Magnetic loss estimates are generated and required motor current is updated for each design mission point.

D. Inverter and Winding Design

The motor inverter and its winding are co-optimized to maximize their combined efficiency subject to the mass constraints specified by the genetic optimizer. First, motor winding wire gauge and strands in hand are selected to minimize combined DC resistive and AC winding loss at various possible turn counts for the motor. Then inverter switching frequency, inverter inductive filter size, inverter switch count, and motor turn count are selected to minimized total loss. DC link capacitors are sized to keep ripple less than 1%. The output of the inverter is required to have less than 5% current ripple. Analytical thermal performance is estimated for the switches and limited to less than 120 C. Inverter design is carried out for steady state at peak mission power including engine out due to the low thermal inertia of the inverter.

E. Short Circuit Analysis

For the fault tolerant motor case, short circuit analysis is carried out both for the initial short and the faulted operation with the phases of the shorted module of the machine shorted together through a large resistance. Simulations are carried out for a short circuit from turn 1 to turn 2 in one phase of one module of the machine. The assumed short circuit resistance is $1 \text{ m}\Omega$. The windings are modeled as an inductance matrix and

resistances. Back EMF is applied as a voltage source. The simulation is carried out in a commercial circuit simulation software. Short circuit current as well as the off nominal current of adjacent coils and phases are extracted from the model.

F. Psuedo Time Stepping FEA

Pseudo time stepping electromagnetic FEA is completed to create higher fidelity loss estimates for the motor. For both the fault tolerant and redundant propulsor cases, the motor is simulated for the faulted cruise condition. For the redundant propulsor motor case, symmetry is used, and magnetic field data is extracted from the first quadrant of the machine and used to create magnetic loss estimates as described in [6]. For the fault tolerant motor case, no symmetry is used, the first quadrant of the machine is assumed to be the quadrant which had a short circuit failure. Field data is extracted from the third quadrant for magnetic loss estimation.

For the fault tolerant motors, the torque and off axis magnetic forces vs rotor position data are extracted from the pseudo time stepping FEA. The loss of torque due to the short circuit currents effect on the rotor is used to recalculate the needed current for the remaining healthy phases to maintain power. The off axis magnetic forces are used to resize the motor bearings and shaft so that they can survive the short circuit fault condition as well as the nominal mission.

G. Inverter Static Thermal FEA

Inverter static thermal FEA is carried out to evaluate the thermal performance of the inverter at each mission design point. From the results of the model a required coolant temperature during cruise operations of the inverter is defined and used to help size the TMS. Geometry and some details of this model can be found in [7].

H. Motor Thermal Mechanical Stress Simulation

Motor coil thermal mechanical stress is evaluated for steady state cruise and climb conditions. One quarter of one slot is simulated as is shown in Fig 5. The shear stress between the winding and the stator iron is evaluated and used to define a linear estimate for that winding's shear stress versus temperature. As is noted in [1], stress limits for coils to have high reliability in UAM application are not well understood at this time. Here max shear stress in the winding is limited to less than 13 MPa assuming delamination of the winding

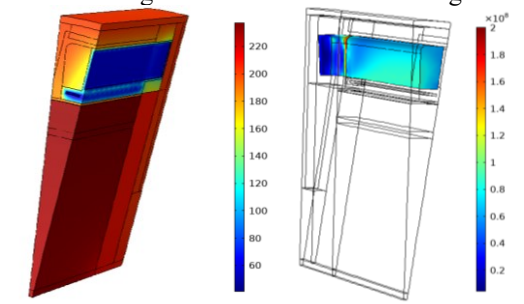


Figure 5 Example Thermal Mechanical Stress Simulation. Left is thermal result in degC. Right is Corresponding Mechanical Stress result in Coil in Pa.

components after some amount of cycling will cause winding failure. The linear function of stress vs winding temperature is used to evaluate the coil stress that results in transient operation of the machine through the transient thermal simulation described in section J. The cruise condition temperature and coil shear stress are used to define the required motor steady state coolant temperature needed for TMS design.

I. Thermal Management System Design

The TMS air to liquid heat exchanger is sized for steady state operation using the coolant temperature limits defined by the motor and inverter static thermal FEA simulations and the losses of all components (gearbox, inverter, and motor). HEATSSPY [9] is used to optimize the TMS and predict its thermal performance throughout the flight profile. After steady state optimization, a thermal reluctance network of the full drivetrain is created and used to simulate thermal performance and coolant temperatures throughout the nominal mission profile. The TMS is resized if any component is predicted to exceed its thermal limitations. Coolant temperatures at the inverter and at the motor are extracted from the simulations and used to define coolant temperature at each mission design point in the transient FEA simulations of those components.

J. Transient Thermal FEA Simulations

Transient thermal FEA simulations are carried out for both the inverter and the motor. Both nominal and faulted/engine out missions are simulated. For the inverter the same geometry as was used in the steady state thermal FEA is used. For redundant propulsor motors the same geometry as was used in the thermomechanical stress simulation is used.

For the fault tolerant motors, a full circumferential model with symmetry at the axial midplane of the machine is used (Fig 6). For the faulted mission, losses corresponding to the faulted operation currents are applied. The module in the first quadrant is assumed to have the fault. The fault is conservatively assumed to occur for 5 seconds at the top of climb before it is sensed and the phases of the module with the fault are shorted together. The short-circuited turns are assumed to be in a coil adjacent to a healthy coil in the second module/quadrant of the

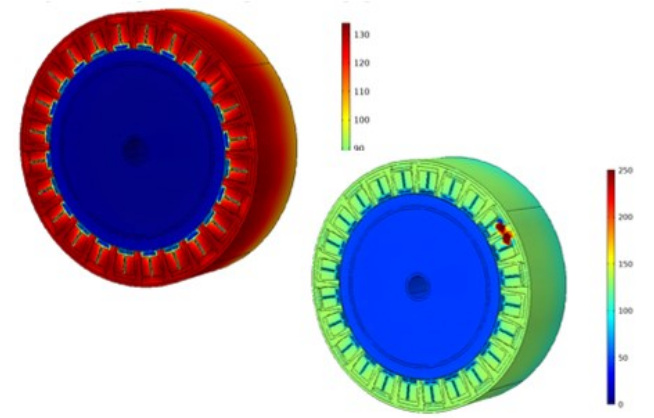


Figure 6 Transient Thermal Simulation Model and Result for Fault Tolerant Motor. Left shows nominal mission result. Right shows faulted result with single turn fault driving the hot spot

machine. Coil temperatures are evaluated for both healthy and faulted conditions in this coil adjacent to the shorted coil.

For both fault tolerant and redundant propulsor motors, the thermal chemical aging of the windings over 10,000 missions is estimated and designs that exceed aging limits are assigned a reduced fitness. The peak coil temperature in the mission is input to the thermal mechanical stress relation defined by the static FEA. Motors for which the shear stress exceeds the allowable are assigned a fitness corresponding to the total drivetrain mass and the stress number predicted here.

K. Fitness Definition

If a drivetrain design passes all the optimization steps its fitness is defined by its mass and total energy loss over the nominal mission. If a design fails at one of the analysis steps, it is assigned a fitness based on the step it made it to. As mentioned previously, designs that make it all the way to transient thermal FEA and fail due to coil mechanical stress are assigned a fitness of the drive train mass and the predicted coil mechanical stress.

IV. RESULTS

Design studies were carried out with relatively small populations of 50 to 60 designs and only to a point that roughly 100-200 closed designs of each type were found. The results correspondingly should not be considered a complete optimization, but a design study for comparison of the topologies explored and understanding of what is required for each design type to close.

Four total studies were completed: the fault tolerant case, a redundant propulsor case assuming 4 vehicle rotors, a redundant propulsor case assuming 8 vehicle rotors, and a case where no faulted operation or engine out condition was included in the design. The 4 rotor case has roughly two times the faulted landing power requirement for the motor as the modules in the fault tolerant case. The 8 rotor case has exactly the same faulted landing condition power as the modules in the fault tolerant case. The no fault case is used as a baseline that is also representative of the limit as number of rotors is increased for the redundant propulsor case.

The best designs of each type found by the design studies are shown in Fig 7. Results are quantified in terms of total drivetrain mass and the nominal full drivetrain mission efficiency of a single propulsor. The 4 rotor case is shown to be roughly 5 to 10 kg heavier than the other cases and significantly less efficient. The bulk of the relative performance loss is in the inverter which has to be significantly oversized to meet the 200 kW faulted landing condition due to its low thermal inertia. Compared to the fault tolerant case with the same rotor count, the redundant 4 rotor case would be 20-40 kg heavier at the vehicle level. It would potentially be more reliable however since it has redundancy for single point failures in the individual propulsors.

The other three design cases are shown to have roughly the same performance. The lowest weight fault tolerant case is shown to be roughly 2 kg heavier than the lightest 8 rotor design and 4 kg heavier than the lightest design with no faulted landing capability. In terms of total drivetrain weight on an aircraft with

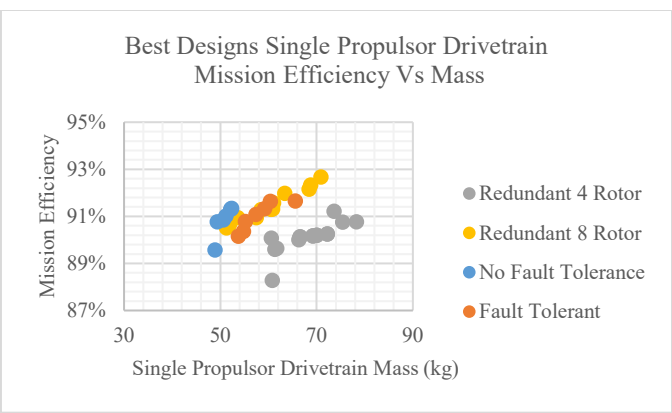


Figure 7 Results of Design Study Showing Pareto Design Found for Each Case

8 rotors, fault tolerant drivetrains would weigh about 16 total kg more than redundant propulsors. The fault tolerant case, apart from the gearbox, would be able to complete engine out flights in an eight rotor configuration since the faulted landing power per module matches between designs. Correspondingly, it would notionally be more reliable since it provides two forms of redundancy for the motor windings and redundancy for the full propulsor as well.

Comparing the design differences between fault tolerant and non-fault tolerant motors that closed, the fault tolerant designs were only able to close with lower motor rpm (lower electrical frequency with fixed pole count in this study) and lower magnet thickness. The motor rotational speed and magnet thickness of all the designs which closed is shown in Fig 8. Both lower RPM and lower magnet thickness correspond to lower back EMF and excitation for fault currents per unit stack length of the machine. The lightest fault tolerant machines did have longer stack lengths than the lightest non-fault tolerant machines to compensate for this lower back EMF per unit length, but those larger stack length correspond to more per turn resistance and inductance for the motors to limit fault currents. Turn counts per phase in the stators were approximately equal.

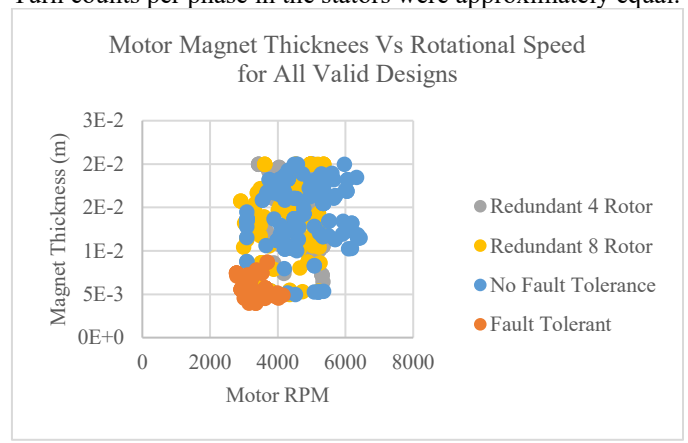


Figure 8 RPM and Magnet Thickness for All Valid Designs Found in Study. Fault Tolerant Machines Shown to Only close for low RPM and small magnet thickness

V. CONCLUSIONS

In this paper an example design study was carried out comparing fault tolerant and redundant motor drivetrains for a tilt rotor UAM application. The results show that for redundant propulsor the cost of redundancy in terms of drivetrain performance is reduced with increased rotor count and that for fault tolerance there is a small performance penalty relative to redundant cases with the same per module faulted motor power. These results are not comprehensive however as the motor topology was held fixed between cases, only one vehicle was studied, and no attempt was made to quantify additional performance changes that would be associated with more redundant propulsors on an aircraft. Future work will focus on expanding these studies to cover more motor topologies and methods of achieving fault tolerance. A quantification of reliability will be included as an optimization objective.

VI. REFERENCES

- T. Tallerico, T. Krantz, M. Valco and J. Salem, "Urban Air Mobility Electric Motor Winding Insulation Reliability: Challenges in the Design and Qualification of High Reliability Electric Motors and NASA's Research Plan," NASA, Cleveland, 2022.
- [2] J. A. Swanke and T. M. Jahns, "Reliability Analysis of a Fault-Tolerant Integrated Modular Motor Drive for an Urban Air Mobility Aircraft Using Markov Chains," *IEEE Transactions on Transportation Electrification*, vol. 8, no. 4, pp. 4523-4533, 2022.
- [3] J. Swanke, D. Bodda, T. Jahns and B. Sarlioglu, "Comparison of Modular PM Propulsion Machines for High Power Density," *IEEE Transportation Electrification Conference and Expo (ITEC)*, pp. 1-7, 2019.
- [4] J. Swanke, H. Zeng and T. Jahns, "Modular Fault-Tolerant Machine Design with Improved Electromagnetic Isolation for Urban Air Mobility (UAM) Aircraft," *IEEE Energy Conversion Congress and Exposition*, pp. 4570-4577, 2021.
- [5] C. Silva, W. Johnson, K. Antcliff and P. D. Michael, "VTOL Urban Air Mobility Concept Vehicles for Technology Development," in AIAA Aviation, Alanta, 2018.
- [6] T. F. Tallerico, "NASA Reference Motor Designs for Electric Vertical Takeoff and Landing Vehicles," in AIAA Propulsion and Energy 2021 Forum, Virtual, 2021.
- [7] T. F. Tallerico, J. Chapman and A. D. Smith, "Preliminary Electric Motor Drivetrain Optimization Studies for Urban Air Mobility Vehicles," in AIAA/IEEE Electric Aircraft Technologies Symposium, Anaheim, 2022.
- [8] T. F. Tallerico, "Genetic Optimization of Planetary Gearboxes Based on Analytical Gearing Equations," NASA, Cleveland, 2022.
- [9] J. Chapman, H. Hasseeb and S. Schnulo, "Thermal Management System Design for Electrified Aircraft Propulsion Concepts," in AIAA Propulsion and Energy 2020 Forum, Virtual, 2020.
- [10] T. Tallerico and A. D. Smith, "Combined Electromagnetic and Thermal Design Optimization Studies of in-Slot Cooling for UAM Electric Motors," in *IEEE Transportation Electrification Conference & Expo* (ITEC), Anaheim, 2022.
- [11] W. Sixel, M. Liu, G. Nellis and B. Sariliogle, "Ceramic 3-D Printed Direct Winding Heat Exchangers for Thermal Management of Concentrated Winding Electric Machines," *IEEE Transactions on Industry Applications*, vol. 57, no. 6, pp. 5829-5840, 2021.